Electronic Supplementary Information to

Coherently and fluorescence-detected two-dimensional electronic spectroscopy: Direct comparison on squaraine dimers

Pavel Malý,[a] Julian Lüttig,[a] Stefan Mueller,[a] Maximilian H. Schreck,[b] Christoph Lambert[b,c] and Tobias Brixner*[a,c]

[a]*Institut für Physikalische und Theoretische Chemie, Universität Würzburg, Am Hubland, 97074 Würzburg, Germany*
[b]*Institut für Organische Chemie, Universität Würzburg, Am Hubland, 97074 Würzburg, Germany*
[c]*Center for Nanosystems Chemistry (CNC), Universität Würzburg, Theodor-Boveri-Weg, 97074 Würzburg, Germany*
brixner@uni-wuerzburg.de

Mixture of independent SQA and SQB molecules

In this section we present F-2DES spectra of a mixture of uncoupled SQA and SQB molecules, first in experiment and then in theory. We unambiguously attribute the spectral correlations (cross peaks) in the absorptive spectra to the presence of exciton–exciton annihilation. In contrast, apparent cross peaks in double-quantum coherence (DQC) and non-rephasing (NR) spectra are present also in the mixture. We show that the reason is the lineshape of the diagonal peaks rather than true spectral correlations.

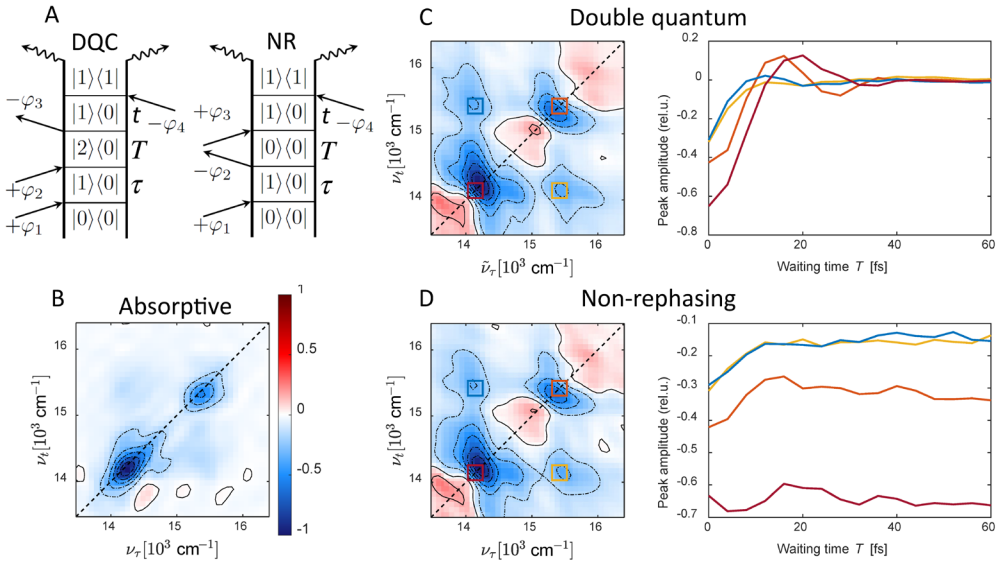

Figure S1 F-2DES of a mixture of SQA and SQB monomers in toluene solution. All 2D spectra are shown at $T = 0$ fs. (A) Response pathways of double-quantum coherence (DQC) and non-rephasing (NR) contributions. When the waiting time T (indicated) is set to zero, there is no difference between these two pathways. (B) Absorptive F-2DES spectrum at $T = 0$ fs, showing essentially no cross peaks. (C) The DQC and (D) NR F-2DES spectra (real parts) show cross peaks as a result of addition of the long spectral tails of the diagonal peaks. Contours of 2D spectra are depicted from -1 to 1 in 12 equidistant steps. Dynamics of selected regions of interest (colored rectangles) over T of the DQC and NR 2D spectra are shown on the right.

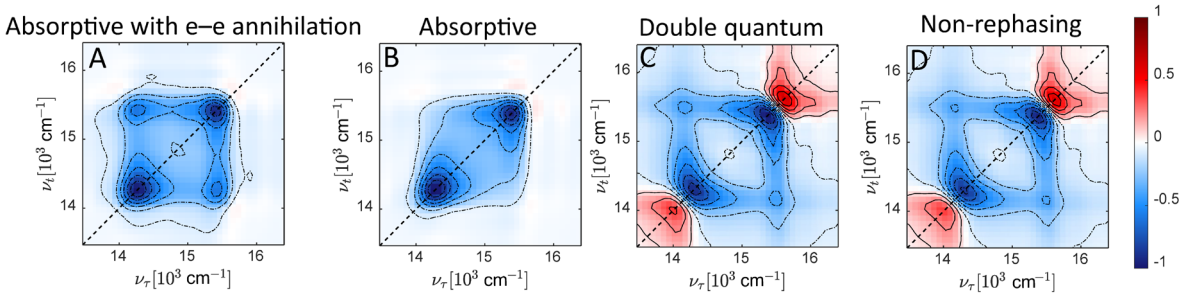

Figure S2 Theoretical F-2DES spectra of a mixture of independent SQA and SQB monomers at waiting time T = 0 fs. All 2D spectra are calculated for uncoupled molecules. (A) In the (hypothetical) presence of exciton–exciton annihilation, the absorptive spectra show pronounced cross peaks. (B) When annihilation is not possible, the cross peaks disappear in the absorptive spectrum. (C) In the non-rephasing and (D) double-quantum coherence spectra, the cross peaks remain even in the absence of exciton–exciton annihilation due to the long tails of the diagonal peaks. These observations agree fully with the experimental data (Fig. S1).

In Fig. S1, we present experimental absorptive F-2DES spectra of a 1:1 mixture of independent SQA and SQB molecules, shown along with the real-valued double-quantum coherence (DQC) and the non-rephasing (NR) 2D spectra. In contrast to the F-2DES spectra of the dSQAB dimers (see Fig. 3 in the main text), the absorptive F-2DES spectrum of the independent mixture of molecules shows practically no spectral correlations (cross peaks). In contrast, the cross peaks in double-quantum coherence (DQC) and nonrephasing (NR) spectra are present also in the mixture of the independent molecules. The waiting time dynamics is discussed in the main text. Briefly, while the NR contributions oscillate around their non-zero value, the DQC signals decay rapidly (in absolute magnitude) within the pulse overlap. In principle, the DQC and NR signals can be distinguished by the oscillating frequency during waiting time dynamics. However, since we are measuring in almost fully rotating frame ($\gamma = 0.1$) and the DQC is quickly damped, this distinction is difficult. We note that the DQC and NR spectra of uncoupled molecules are highly reminiscent of the recently published F-2DES spectra of LH2 of purple bacteria.[1]

We further support our conclusions by calculating F-2DES spectra of uncoupled molecules, which we present in Fig. S2. When we take the molecules as uncoupled ($J_{AB} = 0$) but still (artificially) keep efficient exciton–exciton annihilation ($\Gamma = 1$), we get strong cross peaks in the absorptive spectrum. Only in the absence of any correlations between the molecules ($\Gamma = 2$, no annihilation), these cross peaks disappear, which agrees with the experiment and our previous theoretical work.[2] In the calculated DQC and NR 2D spectra of these uncorrelated molecules, we obtain the cross peaks due to the lineshape of the diagonal peak, again in accordance with our experimental observations. As we verified, by simply adding the 2D spectra for the two molecular species we obtain the same absorptive, DQC and NR 2D spectra. We thus conclude that the cross peaks in the independent mixture originate from the addition of the long tails of the diagonal peaks rather than from electronic correlations.

Excitonic dimer parameters

We used the parameters listed in Table S1 for our excitonic model of the SQA-SQB heterodimers.

Table S1. Parameters for the theoretical simulations (for ease of comparison all quantities were converted to wavenumbers or femtoseconds).

Quantity	**Variable**	**Value**
SQA, SQB transition energy	e_A, e_B	15240 cm^{-1}, 13950 cm^{-1}
Transition energy between first and higher excited monomer state	E_f	12500 cm^{-1}

Electronic coupling between one-exciton transitions for dSQAB-1, dSQAB-2, dSQAB-3	J_{AB}	−350 cm^{-1}, −450 cm^{-1}, −650 cm^{-1}
Scaling of transition coupling into higher excited states	$\xi = J_{fe}/J_{eg}$	0.8
One-exciton transition dipole moment scaling	μ_A, μ_B	1.15, 1.0
Scaling of transition dipole moments to higher excited states	$\mu^f_{A,B}/\mu_{A,B}$	0.66
Scaling of coupling to the bath	ν_A, ν_B	1.0, 1.46
Scaling of coupling to the bath for higher excited states	$\nu^f_{A,B}/\nu_{A,B}$	1.8
Bath reorganization energy	λ	240 cm^{-1}
Bath inverse correlation time	Λ	666 cm^{-1}
Strong vibrational mode parameters: frequency, damping, Huang–Rhys factor	Ω, γ, S	1220 cm^{-1}, 30 cm^{-1}, 0.15
Internal conversion time	τ_{IC}	30 fs
Pulse duration (intensity FWHM), central frequency	t_{pulse}, ω_0	12 fs, 14700 cm^{-1}

The higher excited states $|f_{A,B}\rangle$ are in energy significantly lower than the two-exciton state $|e_A e_B\rangle$, so that they are not directly probed by the laser pulses. This is demonstrated in Fig. S3, where we show the absorption spectrum of the squaraine dimers also in the range of high transition energies, together with the pump and probe spectra, and the spectrum obtained by probing the transitions from the first excited state pumped by the pump pulse.

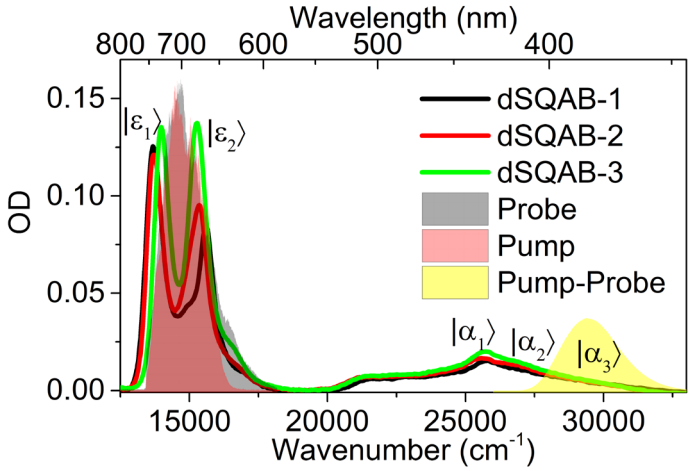

Figure S3 Absorption spectra of the measured squaraine dimers in toluene, in 200 µm cuvette, acquired in a broad spectral range. Denoted are the one-exciton states $|\epsilon_{1,2}\rangle$ and the two-exciton and higher-excited states $|\alpha_n\rangle$. Due to the large energy gap between the higher excited states and the two-exciton state, the double-excited states $|\alpha_n\rangle$ are mostly localized, $|\alpha_1\rangle \approx |f_B\rangle$, $|\alpha_2\rangle \approx |f_A\rangle$, $|\alpha_3\rangle \approx |e_A e_B\rangle$. By shaded regions we denote the pump and probe spectrum, and the 'pump-probe spectrum' obtained as the spectral region accessible by first pumping to the single-excited manifold and subsequent probing. As is apparent from the figure, the higher-excited states $|f_{A,B}\rangle$ are not directly probed.

Influence of laser spectra

In Fig. S4 we demonstrate the effects of the laser spectra on the measured C-2DES and F-2DES spectra. Due to the four-wave-mixing nature of the experiment, the 2D spectra get effectively multiplied by the pump spectrum along the excitation axis and by the pump (probe) spectrum along the detection axis

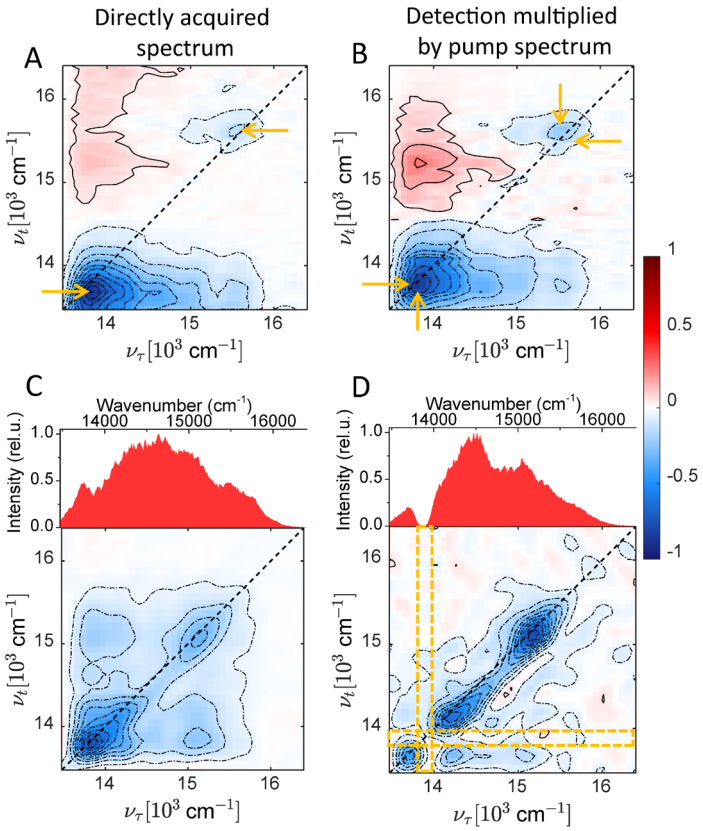

Figure S4 Influence of laser spectra on the measured 2DES spectra. Top: C-2DES spectra of dSQAB-1 acquired as differential (pumped–unpumped) spectra in the pump–probe geometry. (A) Directly acquired spectrum, as presented in the main manuscript. The yellow arrows next to the diagonal peaks denote the peak shift from the diagonal as a result of the pump spectrum pulling. (B) Multiplication by the pump spectrum along the detection axis brings the peaks back to the diagonal. Bottom: F-2DES spectra of dSQAB-3 dimer acquired using (C) a spectrum without and (D) with a spectral hole. As indicated by the yellow rectangles, the hole in the laser spectrum leads to 'trenches' in the measured 2D spectrum.

for F-2DES (C-2DES). In particular, it can be shown that under the assumption of time-ordered pulses, the third-order signal field in C-2DES can be expressed as

$$E_{\mathrm{sig}}(\omega_t,\omega_T,\omega_\tau) \propto i\frac{\omega_t}{n(\omega_t)}S^{(3)}(\omega_t,\omega_T,\omega_\tau)E_{\mathrm{P}}(\omega_\tau)E_{\mathrm{P}}^*(\omega_\tau-\omega_T)E_{\mathrm{Pr}}(\omega_t-\omega_T), \qquad \text{(S1)}$$

wherein $E_{\mathrm{P}}(\omega)$ is the spectral field amplitude of the pump pulse and $E_{\mathrm{Pr}}(\omega)$ that of the probe pulse. In the following we will consider slowly-varying dynamics in the waiting time, such as population dynamics, neglecting ω_T against ω_t and ω_τ. We also, for simplicity, assume the polarization of all electric fields to be parallel, so that it is enough to write the fields and dipoles as scalars. Now, in pump–probe geometry the differential transmission signal is evaluated[1],

$$\frac{\Delta T}{T} = \frac{I_{\mathrm{P-Pr}} - I_{\mathrm{Pr}}}{I_{\mathrm{Pr}}} = \frac{2\mathrm{Re}\{E_{\mathrm{sig}}\cdot E_{\mathrm{Pr}}^*\} + I_{\mathrm{sig}}}{I_{\mathrm{Pr}}}, \qquad \text{(S2)}$$

[1] Alternatively transient absorption may be defined as $-\Delta\mathrm{OD} = \log(I_{\mathrm{P-Pr}}) - \log(I_{\mathrm{Pr}})$, which leads to the same expression when using $\log\left(1+\frac{2\mathrm{Re}\{E_{\mathrm{sig}}\cdot E_{\mathrm{Pr}}^*\}}{I_{\mathrm{Pr}}}\right) \approx \frac{2\mathrm{Re}\{E_{\mathrm{sig}}\cdot E_{\mathrm{Pr}}^*\}}{I_{\mathrm{Pr}}}$.

wherein $I_{\mathrm{P-Pr}}$ is the measured probe beam intensity measured with the pump pulse also present, I_{Pr} is the probe intensity without the pump pulse hitting the sample, and I_{sig} is the intensity of the signal itself. Neglecting I_{sig} and inserting the expression for E_{sig} from Eq. (S1) we get for the absorptive spectrum with slowly-varying waiting-time dynamics

$$\text{C-2DES}(\omega_t, \omega_T, \omega_\tau) \propto \frac{\omega_t}{n(\omega_t)} \mathrm{Re}\{S^{(3)}(\omega_t, \omega_T, \omega_\tau)\} I_P(\omega_\tau). \quad \text{(S3)}$$

Clearly, the probe spectrum multiplication along the ω_t axis gets removed by the differential acquisition. The spectrum thus remains multiplied by the pump spectrum along ω_τ. This we demonstrate in Fig. S4A and B, where we show the C-2DES spectrum of dSQAB-1, which has its two peaks close to the edges of our laser pulse spectra. As a result of the asymmetric multiplication, due to the remaining "pulling" effect of the pump spectrum, the peaks appear off-diagonal (Fig. S4A).[3] This can be remedied by multiplying the 2D spectra by the pump pulse spectrum $I_{\mathrm{P}}(\omega)$ along the detection axis ω_t, effectively pulling the peaks back (Fig. S4B). A more logical way to "correct" the 2D spectra would be to divide them by the pump spectrum along the excitation axis according to Eq. (S3). However, in practice this does not work well, because the division over-emphasizes the spectral edges where the experimental spectrum has low intensity and therefore low signal-to-noise ratio.

In a similar way one can show that the absorptive F-2DES spectrum under the assumption of time-ordered pulses and slowly-varying waiting-time dynamics will be proportional to

$$\text{F-2DES}(\omega_t, \omega_T, \omega_\tau) \propto \mathrm{Re}\{S^{(4)}(\omega_t, \omega_T, \omega_\tau)\} I_{\mathrm{P}}(\omega_\tau) I_{\mathrm{Pr}}(\omega_t). \quad \text{(S4)}$$

The F-2DES spectrum is thus effectively multiplied by the pump spectrum along the excitation axis and by the probe spectrum along the detection axis. We note that in our and typical other experiments the pump and probe spectra are the same. In Fig. S4C and D we show the effective multiplication of the F-2DES spectra of dSQAB-3 by the pulse spectrum by measuring with a spectral hole (produced by amplitude shaping with the pulse shaper). Compared to the unshaped case (Fig. S4C), such a hole in a pump spectrum produces "trenches" in the F-2DES spectra both along the excitation and the detection axis (Fig. S4D).

In the same fashion as the clear cases discussed here, all spectral features, such as modulated spectra, manifest in measured C-2DES and F-2DES spectra. These effects should not be underestimated, in particular when a detailed analysis of peak shapes is of interest. We note that in deriving the simple expressions above we used the severe and somewhat unrealistic assumption of time-ordered pulses. Inevitably, for finite pulses of appreciable spectral modulation the time ordering will be an issue, producing yet different effects in the 2D spectra. Such effects were studied in literature.[3,4] It might be interesting to investigate in more detail how the time-ordering or spectral-modulation effects lead to changes in the 2D spectra, whether it is possible to disentangle them, and if one could obtain corrected spectra, getting closer to the desired response function.

Experimental setup

In Fig. S5 we show the experimental setup, described in detail in the 'Experimental and Theoretical Methods' section in the main text. Note that switching between C-2DES and F-2DES requires only a flip of a mirror.

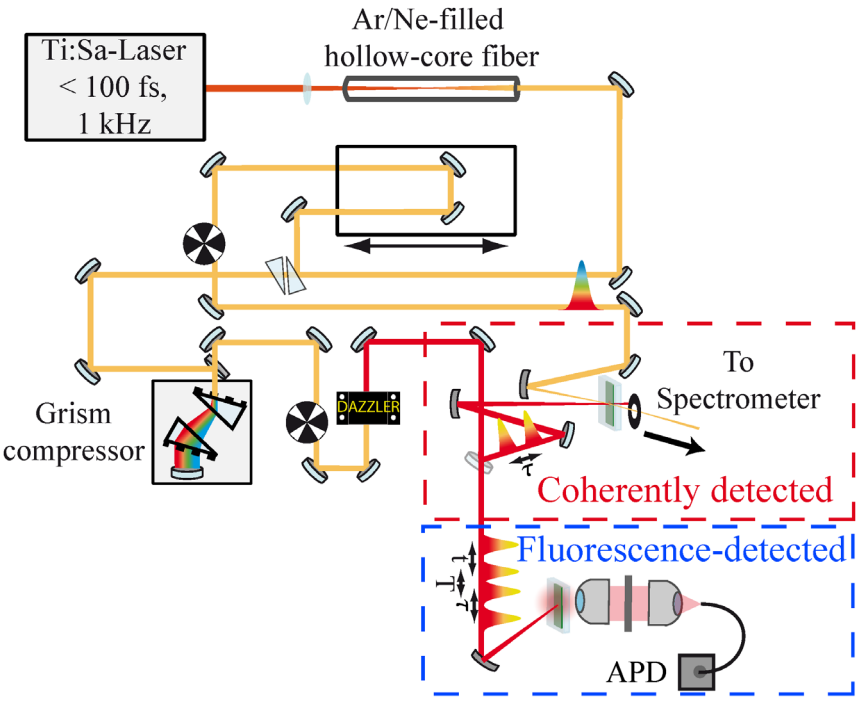

Figure S5 Experimental setup scheme.

Waiting time dynamics

Here we show in Fig. S6 the rephasing F-2DES spectra and the lower cross peak oscillatory traces, which we used to extract the spectrum of the waiting time oscillations shown in Fig. 6D of the main text.

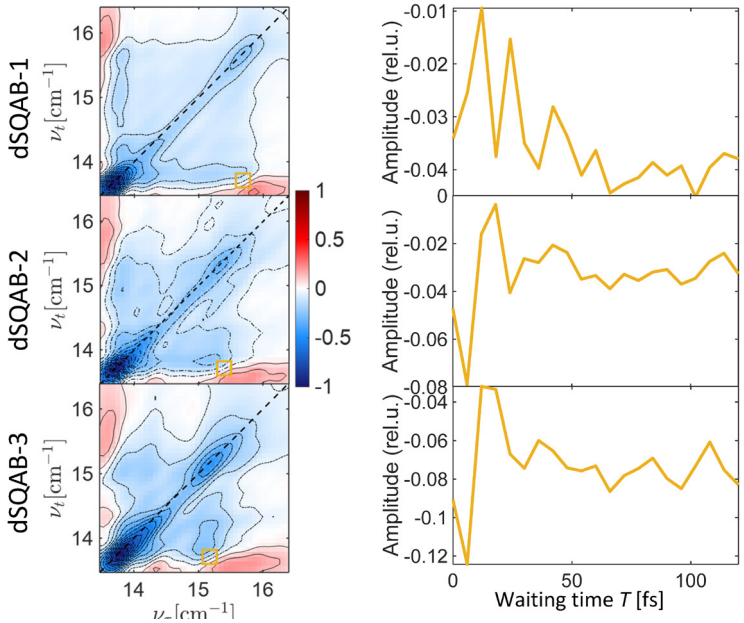

Figure S6 Real rephasing (photon echo) spectra of the three squaraine dimers, and the oscillatory dynamics of the lower cross peak, evaluated in the region of interest marked in the 2D spectra.

For completeness, we also present here in Fig. S7 the full dynamics of the real absorptive spectra for all dimers, both for C-2DES and F-2DES.

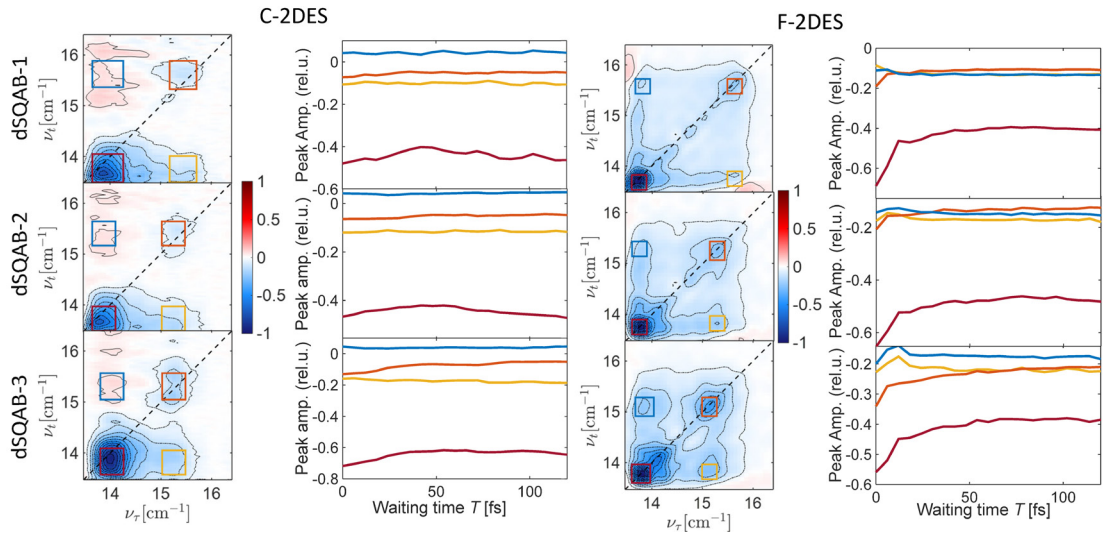

Figure S7 Full set of the time-zero real absorptive spectra and the peak dynamics in the waiting time *T*, for C-2DES (left) and F-2DES (right), with regions of interest marked in the 2D spectra with the corresponding colors.

Squaraine dimer synthetic procedure

All synthetic preparations were performed in standard glassware. The chemicals used were purchased from commercial suppliers and utilised without further purification. Reactions under nitrogen atmosphere (dried over Sicapent form Merck; oxygen was removed by copper catalyst R3-11 from BASF) were carried out in oven-dried glass ware with solvents that were dried according to literature procedures and stored under nitrogen. Silica gel 32 - 64 µm was used for flash chromatography.

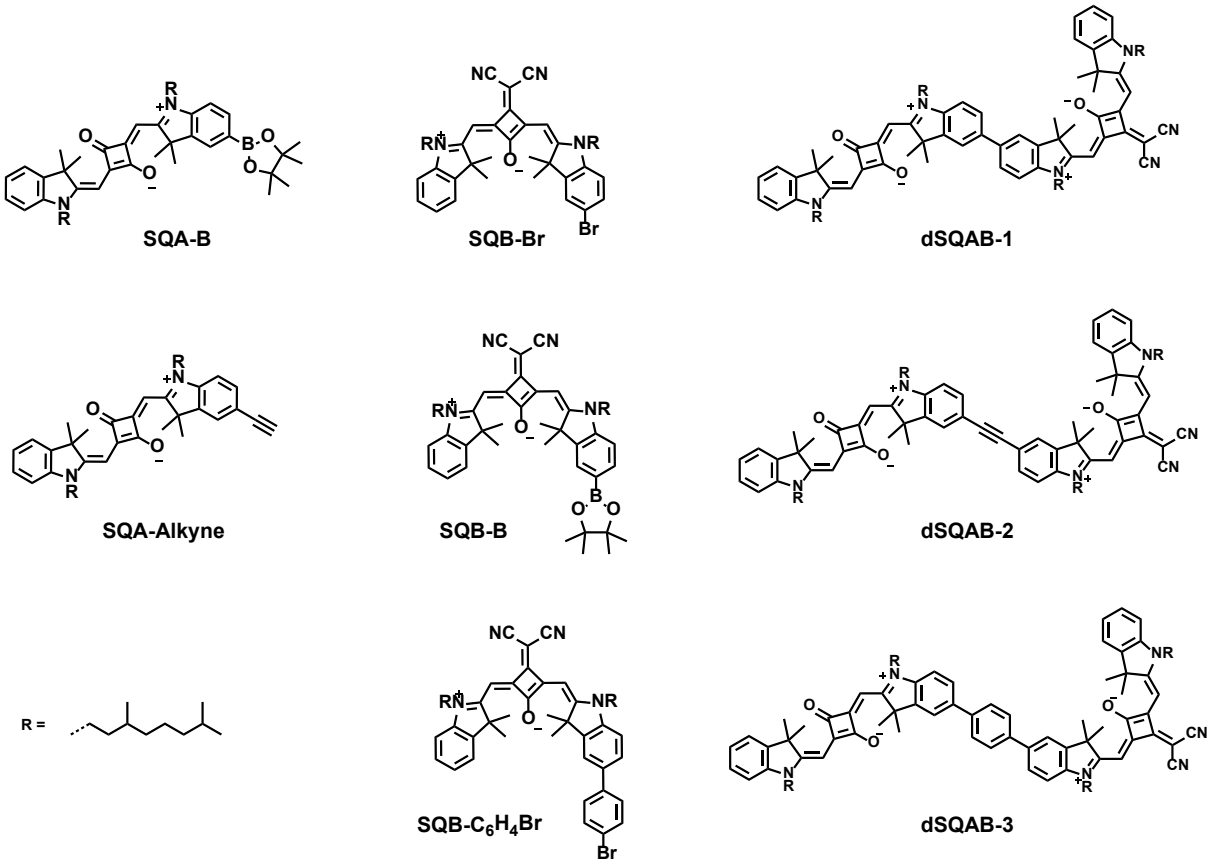

Figure S8 Precursors **SQA-B**, **SQA-Alkyne**, **SQB-Br**, **SQB-B**, **SQB-C_6H_4Br** and squaraine heterodimers **dSQAB-1**, **dSQAB-2** and **dSQAB-3**.

Compounds **SQA-B**[5], **SQA-Alkyne**[5], **SQB-Br**[6], **SQB-B**[7] and **dSQAB-1**[8] (cf. Figure S8) were synthesized according to given literature.

Synthesis of the dSQAB-2 dimer

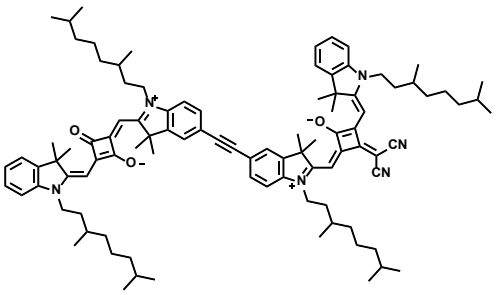

Under a nitrogen atmosphere squaraine **SQB-Br**[6] (34.0 mg, 42.3 µmol) was dissolved in dry NEt_3 (10 ml). The dark green solution was degassed in a gentle stream of nitrogen for 20 min. CuI (239 µg, 1.25 µmol) and $Pd(PPh_3)_2Cl_2$ (881 µg, 1.26 µmol) were subsequently added and the mixture was heated to 60 °C. A degassed solution of squaraine **SQA-Alkyne**[5] (44.0 mg, 62.8 µmol) in dry NEt_3 (10 ml) was carefully added dropwise over a period of 45 min. After complete addition the reaction mixture was heated to reflux for 2 h. The solvent was removed *in vacuo* and the residue purified by flash chromatography (DCM/MeOH = 99:1) and subsequent preparative GPC ($CHCl_3$).

Yield: 16.0 mg (11.2 µmol, 26 %) of a shiny red solid.

$C_{97}H_{126}N_6O_3$ [1424.08]

^{1}H-NMR (400.1 MHz, CD_2Cl_2):

δ [ppm] = 7.57-7.47 (-, 4H, 4 × C*H*), 7.45-7.30 (-, 4H, 4 × C*H*), 7.25 (ddd, ^3J = 7.5 Hz, ^3J = 7.5 Hz, ^4J = 0.7 Hz, 1H, C*H*), 7.22-7.15 (m, 1H, C*H*), 7.11 (d, ^3J = 7.9 Hz, 1H, C*H*), 7.18-6.99 (-, 2H, 2 × C*H*), 6.96 (d, ^3J = 7.1 Hz, 1H, C*H*), 6.52 (s, 1H, C*H*), 6.46 (s, 1H, C*H*), 5.96 (s, 1H, C*H*), 5.91 (s, 1H, C*H*), 4.17-3.86 (-, 8H, 4 × NCH_2), 1.86-1.71 (-, 28H, 4 × NCH_2CH, 8 × CH_3), 1.70-1.58 (-, 8H, 4 × C*H*, 4 × NCH_2CH), 1.56-1.45 (-, 4H, 4 × C*H*), 1.44-1.11 (-, 24H, 12 × CH_2), 1.11-1.05 (-, 6H, 2 × CH_3), 1.05-1.00 (-, 6H, 2 × CH_3), 0.90-0.83 (-, 24H, 8 × CH_3).

^{13}C-NMR (100.6 MHz, CD_2Cl_2):

δ [ppm] = 182.2 (2 × quart), 180.7 (quart), 179.6 (quart), 173.4 (quart), 173.0 (quart), 171.1 (quart), 170.8 (quart), 168.4 (quart), 168.0 (quart), 167.7 (quart), 166.0 (quart), 143.2 (quart), 143.1 (2 × quart), 142.8 (quart), 142.8 (quart), 142.7 (quart), 142.3 (quart), 142.2 (quart), 132.0 (tert), 131.9 (tert), 128.4 (tert), 128.2 (tert), 125.8 (tert), 125.6 (tert), 125.3 (tert), 124.4 (tert), 122.8 (tert), 122.7 (tert), 119.2 (quart), 119.07 (quart), 118.5 (quart), 118.0 (quart), 110.8 (tert), 110.3 (tert), 110.1 (tert), 109.5 (tert), 89.9 (quart), 89.8 (tert), 89.73 (quart), 89.66 (tert), 87.5 (tert), 87.3 (tert), 50.1 (quart), 49.9 (quart), 49.4 (quart), 49.1 (quart), 43.5 (sec), 43.3 (sec), 42.6 (sec), 42.4 (sec), 40.8 (quart), 39.54 (2 × sec), 39.53 (2 × sec), 37.48 (2 × sec), 37.47 (2 × sec), 34.5 (sec), 34.3 (sec), 34.2 (sec), 34.0 (sec), 31.5 (2 × tert), 31.3 (2 × tert), 28.39 (2 × tert), 28.38 (2 × tert), 27.2 (2 × prim)*, 27.0 (2 × prim)*, 26.9 (prim)*, 26.8 (prim)*, 26.55 (prim)*, 26.52 (prim)*, 25.1 (2 × sec), 25.03 (sec), 25.02 (sec), 22.825 (prim), 22.819 (prim), 22.74 (prim), 22.73 (prim), 19.79 (prim), 19.78 (2 × prim), 19.75 (prim).

* The signal of the primary C-atoms splits into two signals of equal intensity.

ESI-MS pos (high resolution): $[M^{\cdot+}]$

calc.: 1423.99186 m/z

found: 1423.99209 m/z Δ = 0.16 ppm

SQB-C_6H_4-Br

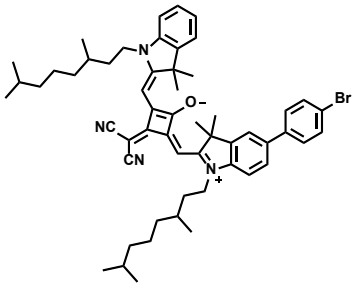

Functionalized squaraine dye **SQB-B**[7] (128 mg, 150 µmol) and 1,4-dibromobenzene (35.0 mg, 148 µmol) were dissolved in peroxide-free THF (10 ml) under a nitrogen atmosphere. An aqueous solution of Na_2CO_3 (1 M, 451 µl, 451 µmol) was added and the mixture was purged in a gentle stream of nitrogen for 15 min. $Pd(PPh_3)_4$ (17.0 mg, 14.7 µmol) was added and the reaction was heated at 85 °C in a sealed tube for 2 d. The solvent was removed *in vacuo* and the residue purified by flash chromatography (DCM/MeOH = 99:1) and subsequent preparative recycling GPC ($CHCl_3$). After purification, the compound was dissolved in a small amount of DCM and dripped into an excess of *n*-hexane. The precipitate formed was filtered off and dried under high vacuum, respectively.

Yield: 47.0 mg (53.4 µmol, 36 %) of a green solid.

$C_{55}H_{67}BrN_4O$ [880.05]

^{1}H-NMR (400.1 MHz, CD_2Cl_2):

δ [ppm] = 7.65-7.54 (-, 4H, 4 × C*H*), 7.54-7.44 (-, 2H, 2 × C*H*), 7.44-7.31 (-, 2H, 2 × C*H*), 7.31-6.96 (-, 3H, 3 × C*H*), 6.82-6.03 (-, 2H, 2 × C*H*), 4.56-3.50 (-, 4H, 2 × NCH_2), 1.90-1.72 (-, 14H, 2 × NCH_2CH, 4 × CH_3), 1.72-1.58 (-, 4H, 2 × NCH_2CH, 2 × C*H*), 1.58-1.46 (-, 2H, 2 × C*H*), 1.46-1.10 (-, 12H, 6 × CH_2), 1.04 (d, ^3J = 6.4 Hz, 3H, CH_3), 1.03 (d, ^3J = 6.4 Hz, 3H, CH_3), 0.90-0.82 (-, 12H, 4 × CH_3).

^{13}C-NMR (100.6 MHz, CD_2Cl_2):

δ [ppm] = 173.5 (quart), 172.5 (quart), 171.5 (quart), 167.9 (quart), 167.2 (quart), 166.3 (quart), 143.6 (quart), 143.0 (quart), 142.3 (quart), 142.2 (quart), 139.9 (quart), 136.7 (quart), 132.3 (tert), 128.9 (tert), 128.4 (tert), 127.2 (tert), 125.1 (tert), 122.6 (tert), 121.7 (quart), 121.1 (tert), 119.1 (2 × quart), 110.7 (tert), 110.6 (tert), 89.6 (tert), 89.5 (tert), 50.0 (quart), 49.8 (quart), 43.40 (sec), 43.35 (sec), 40.7 (quart), 39.5 (2 × sec), 37.5 (2 × sec), 34.40 (sec), 34.37 (sec), 31.3 (2 × tert), 28.4 (2 × tert), 26.9 (prim)*, 26.8 (prim)*, 26.61 (prim)*, 26.58 (prim)*, 25.03 (sec), 25.02 (sec), 22.8 (2 × prim)*, 22.7 (2 × prim)*, 19.82 (prim), 19.78 (prim).

* The signals of the primary C-atoms split into two signals of equal intensity.

MALDI-MS pos: [M^{+}]

calc.: 880.449 m/z

found: 880.404 m/z

Synthesis of the dSQAB-3 dimer

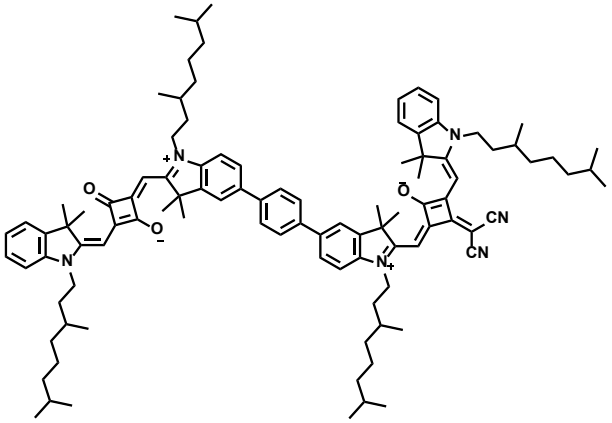

Functionalized squaraine dye **SQA-B**[5] (25.0 mg, 31.1 µmol) and squaraine **SQB-C_6H_4-Br** (36.0 mg, 40.9 µmol) were dissolved in peroxide-free THF (7 ml) under a nitrogen atmosphere. An aqueous solution of Na_2CO_3 (1 M, 93.0 µl, 93.0 µmol) was added and the mixture was purged in a gentle stream of nitrogen for 15 min. $Pd(PPh_3)_4$ (3.60 mg, 3.12 µmol) was added and the reaction was heated at 85 °C in a sealed tube for 2 d. The solvent was removed *in vacuo* and the residue purified by flash chromatography (DCM/MeOH = 99:1) and subsequent preparative recycling GPC ($CHCl_3$). Finally, the product was dissolved in a small amount of DCM and dripped into an excess of *n*-hexane. The mixture was allowed to stand in the refrigerator at 4 °C overnight. The precipitate formed was filtered off and dried under high vacuum.

Yield: 10.0 mg (6.77 µmol, 22 %) of a green solid.

$C_{101}H_{130}N_6O_3$ [1476.16]

^{1}H-NMR (400.1 MHz, CD_2Cl_2):

δ [ppm] = 7.77-7.70 (-, 4H, 4 × C*H*), 7.69-7.60 (-, 4H, 4 × C*H*), 7.43-7.29 (-, 4H, 4 × C*H*), 7.22 (ddd, ^3J = 7.5 Hz, ^3J = 7.5 Hz, ^4J = 0.7 Hz, 1H, C*H*), 7.19-7.12 (-, 2H, 2 × C*H*), 7.12-7.05 (-, 2H, 2 × C*H*), 7.05-6.96 (m, 1H, C*H*), 6.497 (s, 1H, C*H*), 6.493 (s, 1H, C*H*), 6.08-5.80 (-, 2H, 2 × C*H*), 4.20-3.89 (-, 8H, 4 × NCH_2), 1.90-1.71 (-, 28H, 4 × NCH_2CH, 8 × CH_3), 1.71-1.60 (-, 8H, 4 × NCH_2CH, 4 × C*H*), 1.59-1.47 (-, 4H, 4 × C*H*), 1.47-1.13 (-, 24H, 12 × CH_2), 1.12-1.07 (-, 6H, 2 × CH_3), 1.05 (d, ^3J = 6.4 Hz, 3H, CH_3), 1.03 (d, ^3J = 6.4 Hz, 3H, CH_3), 0.90-0.84 (-, 24H, 8 × CH_3).

^{13}C-NMR (100.6 MHz, CD_2Cl_2):

δ [ppm] = 182.0 (2 × quart), 181.3 (quart), 180.1 (quart), 173.5 (quart), 172.3 (quart), 171.6 (quart), 170.4 (quart), 169.2 (quart), 167.9 (quart), 167.0 (quart), 166.4 (quart), 143.7 (quart), 143.4 (quart), 142.9 (quart), 142.8 (quart), 142.7 (quart), 142.5 (quart), 142.3 (quart), 142.0 (quart), 141.4 (quart), 139.9 (quart), 139.6 (quart), 137.4 (quart), 128.4 (2 × tert), 127.7 (2 × tert), 127.2 (2 × tert), 125.0 (2 × tert), 122.6 (2 × tert), 121.2 (2 × tert), 119.2 (2 × quart), 110.7 (tert), 110.6 (tert), 109.9 (tert), 109.8 (tert), 89.6 (tert), 89.5 (tert), 87.2 (tert), 87.0 (tert), 49.9 (2 × quart), 49.8 (2 × quart), 43.4 (2 × sec), 43.3 (2 × sec), 40.6 (quart), 39.54 (2 × sec), 39.53 (2 × sec), 37.50 (2 × sec), 37.48 (2 × sec), 34.41 (2 × sec), 34.39 (2 × sec), 31.5 (2 × tert), 31.3 (2 × tert), 28.40 (tert), 28.39 (tert), 28.38 (tert), 28.37 (tert), 26.86 (prim), 26.82 (prim), 26.65 (prim), 26.62 (prim), 25.1 (2 × sec), 25.04 (sec), 25.02 (sec), 22.8 (2 × prim), 22.7 (2 × prim), 19.83 (2 × prim), 19.79 (2 × prim).

ESI-MS pos (high resolution): $[MH^{\cdot+}]$

calc.: 1477.0310 m/z

found: 1477.0294 m/z Δ = 1.08 ppm

References

1 K. J. Karki, J. Chen, A. Sakurai, Q. Shi, A. T. Gardiner, O. Kühn, R. J. Cogdell and T. Pullerits, *Chem. Sci.*, 2019, **10**, 7923–7928.

2 P. Malý and T. Mančal, *J. Phys. Chem. Lett.*, 2018, **9**, 5654–5659.

3 V. Perlík, J. Hauer and F. Šanda, *JOSA B*, 2017, **34**, 430–439.

4 P. F. Tekavec, J. A. Myers, K. L. M. Lewis, F. D. Fuller and J. P. Ogilvie, *Opt. Express*, 2010, **18**, 11015–11024.

5 M. Schreck, Dissertation, University of Würzburg, 2018.

6 H. Ceymann, M. Balkenhohl, A. Schmiedel, M. Holzapfel and C. Lambert, *Phys. Chem. Chem. Phys.*, 2016, **18**, 2646–2657.

7 H. Ceymann, A. Rosspeintner, M. H. Schreck, C. Mützel, A. Stoy, E. Vauthey and C. Lambert, *Phys. Chem. Chem. Phys.*, 2016, **18**, 16404–16413.

8 M. I. S. Röhr, H. Marciniak, J. Hoche, M. H. Schreck, H. Ceymann, R. Mitric and C. Lambert, *J. Phys. Chem. C*, 2018, **122**, 8082–8093.